Letter

Universal optical polarizability for plasmonic nanostructures

Tigran V. Shahbazyan
Department of Physics, Jackson State University, Jackson, Mississippi 39217, USA

(Received 6 January 2023; revised 11 April 2023; accepted 2 June 2023; published 21 June 2023)

We develop an analytical model for calculation of optical spectra for metal nanostructures of arbitrary shape supporting localized surface plasmons (LSPs). For plasmonic systems with characteristic size below the diffraction limit, we obtain an explicit expression for optical polarizability that describes the lineshape of optical spectra solely in terms of the metal dielectric function and LSP frequency. The amplitude of the LSP spectral band is determined by the effective system volume that, for long-wavelength LSPs, can significantly exceed the physical volume of metal nanostructure. Within the quasistatic approach, we derive the exact LSP Green's function and establish general spectral properties of LSPs, including the distribution and oscillator strength of the LSP states. These results can be used to model or interpret the experimental spectra of plasmonic nanostructures and to tune their optical properties for various applications.

DOI: 10.1103/PhysRevA.107.L061503

I. INTRODUCTION

Localized surface plasmons (LSPs) are collective electron excitations resonantly excited by incident light in metal nanostructures with characteristic size below the diffraction limit [1–3]. Optical interactions between the LSPs and excitons in dye molecules or semiconductors underpin numerous phenomena in the plasmon-enhanced spectroscopy, such as surface-enhanced Raman scattering [4], plasmon-enhanced fluorescence and luminescence [5–12], strong exciton-plasmon coupling [13–23], and plasmonic lasers (spasers) [24–27]. Optical properties of metal nanostructures of various sizes and shapes are of critical importance for numerous plasmonics applications [28–30], and were therefore extensively studied experimentally and theoretically [31–37]. The optical polarizability tensor $\boldsymbol{\alpha}(\omega)$ of a plasmonic nanostructure determines its response to an incident electromagnetic (EM) field $\boldsymbol{E}_{\rm in}e^{-i\omega t}$, where ω is the incident field frequency and, at the same time, defines the optical interactions between the LSPs and excitons. If the characteristic system size is much smaller than the radiation wavelength, so that $\boldsymbol{E}_{\rm in}$ is nearly uniform on the system scale, the induced dipole moment of a plasmonic nanostructure has the form $\boldsymbol{p}(\omega)=\boldsymbol{\alpha}(\omega)\boldsymbol{E}_{\rm in}$, where $\boldsymbol{\alpha}(\omega)$ can be calculated, with a good accuracy, within the quasistatic approach [3]. Fully analytical models for $\boldsymbol{\alpha}(\omega)$ have long been available for systems of highly symmetric shapes, such as spherical, ellipsoidal, or cylindrical structures [32]. For example, a metal nanosphere of radius a placed in the air is characterized by the scalar polarizability:

$$\alpha(\omega)=a^3\,\frac{\varepsilon(\omega)-1}{\varepsilon(\omega)+2}, \tag{1}$$

where $\varepsilon(\omega)=\varepsilon'(\omega)+i\varepsilon''(\omega)$ is a complex dielectric function of the metal. For more complicated shapes, several models have been suggested as well which, however, contain some parameters to be calculated numerically [32–36].

On the other hand, due to uncertainties in the shape and size of actual structures explored in the experiment, the analytical or numerical models describing *both* the LSP frequency and the lineshape of optical spectra, as Eq. (1) does, are not even necessary. Typically, the spectral position of the LSP resonance peak is measured with a reasonably high accuracy, and so the main challenge is to describe or interpret the spectral lineshape [37,38]. Here, we present an analytical model describing accurately the optical spectra of plasmonic nanostructures of *arbitrary* shape with LSP frequencies treated as *input* parameters.

Specifically, the optical polarizability tensor of a small metal nanostructure supporting LSP resonance at a frequency ω_n has the form $\boldsymbol{\alpha}_n(\omega)=\alpha_n(\omega)\boldsymbol{e}_n\boldsymbol{e}_n$, where

$$\alpha_n(\omega)=V_n\,\frac{\varepsilon(\omega)-1}{\varepsilon(\omega)-\varepsilon'(\omega_n)} \tag{2}$$

is the scalar polarizability, $\boldsymbol{e}_n$ is the unit vector for LSP mode polarization, and $V_n=V_{\rm m}|\chi'(\omega_n)|s_n$ is the effective volume. Here, $V_{\rm m}$ is the metal volume, $\chi'(\omega)=[\varepsilon'(\omega)-1]/4\pi$ is the real part of susceptibility (we use Gaussian units), and the parameter $s_n\leqslant 1$ depends on the system geometry. Thus, for any geometry, the lineshape of optical spectra is determined only by the metal dielectric function and the LSP frequency, while the spectral peak amplitude depends on the system effective volume. The polarization (2) can be extended to larger systems by including the LSP radiation damping.

To obtain Eq. (2), we employed the LSP Green's-function approach in the quasistatic regime [39–42]. Within this approach, we have also established several exact relations characterizing the distribution of LSP states.

II. LSP GREEN'S FUNCTION

We consider a metal nanostructure supporting a LSP that is localized at a length scale much smaller than the radiation wavelength. In the absence of retardation effects, each region of the structure, metallic or dielectric, is characterized by the

dielectric function $\varepsilon_i(\omega)$, so that the full dielectric function is $\varepsilon(\omega,\boldsymbol{r})=\sum_i\theta_i(\boldsymbol{r})\varepsilon_i(\omega)$, where $\theta_i(\boldsymbol{r})$ is the unit step function that vanishes outside of the region volume V_i. We assume that dielectric regions' permittivities are constant, and adopt $\varepsilon(\omega)$ for the metal region. The LSP modes are defined by the lossless Gauss equation as [3]

$$\nabla\cdot[\varepsilon'(\omega_n,\boldsymbol{r})\nabla\Phi_n(\boldsymbol{r})]=0, \tag{3}$$

where $\Phi_n(\boldsymbol{r})$ and $\boldsymbol{E}_n(\boldsymbol{r})=-\nabla\Phi_n(\boldsymbol{r})$ are the mode's potential and electric field, which we chose real. Note that the eigenmodes of Eq. (3) are orthogonal in each region (see Supplemental Material [39]): $\int dV_i\boldsymbol{E}_n(\boldsymbol{r})\cdot\boldsymbol{E}_{n'}(\boldsymbol{r})=\delta_{nn'}\int dV_i\boldsymbol{E}_n^2(\boldsymbol{r})$.

The EM dyadic Green's function $\boldsymbol{D}(\omega;\boldsymbol{r},\boldsymbol{r}')$ satisfies (in the operator form) $\nabla\times\nabla\times\boldsymbol{D}-(\omega^2/c^2)\varepsilon\boldsymbol{D}=(4\pi\omega^2/c^2)\boldsymbol{I}$, where $\boldsymbol{I}$ is the unit tensor, while the longitudinal part of $\boldsymbol{D}$ is obtained by applying the operator ∇ to both sides. In the near field, we switch to the scalar Green's function for the potentials $D(\omega;\boldsymbol{r},\boldsymbol{r}')$, defined as $\boldsymbol{D}(\omega;\boldsymbol{r},\boldsymbol{r}')=\nabla\nabla' D(\omega;\boldsymbol{r},\boldsymbol{r}')$, which satisfies [compare to Eq. (3)]

$$\nabla\cdot[\varepsilon(\omega,\boldsymbol{r})\nabla D(\omega;\boldsymbol{r},\boldsymbol{r}')]=4\pi\delta(\boldsymbol{r}-\boldsymbol{r}'). \tag{4}$$

We now adopt the decomposition $D=D_0+D_{\rm LSP}$, where $D_0(\boldsymbol{r}-\boldsymbol{r}')=-|\boldsymbol{r}-\boldsymbol{r}'|^{-1}$ is the free-space Green's function and $D_{\rm LSP}(\omega;\boldsymbol{r},\boldsymbol{r}')$ is the LSP contribution. The latter is expanded over the eigenmodes of Eq. (3) as [39–42]

$$D_{\rm LSP}(\omega;\boldsymbol{r},\boldsymbol{r}')=\sum_n D_n(\omega)\Phi_n(\boldsymbol{r})\Phi_n(\boldsymbol{r}'), \tag{5}$$

where the coefficients $D_n(\omega)$ have the form

$$D_n(\omega)=\frac{4\pi}{\int dV\boldsymbol{E}_n^2(\boldsymbol{r})}-\frac{4\pi}{\int dV\varepsilon(\omega,\boldsymbol{r})\boldsymbol{E}_n^2(\boldsymbol{r})}. \tag{6}$$

The first term in Eq. (6) ensures the boundary condition for $\varepsilon=1$ and will be omitted in the following. While the expansion in Eq. (5) runs over the eigenmodes of the lossless Gauss equation (3), the coefficients D_n depend on complex $\varepsilon(\omega,\boldsymbol{r})=\varepsilon'(\omega,\boldsymbol{r})+i\varepsilon''(\omega,\boldsymbol{r})$ [39]. Accordingly, the LSP dyadic Green's function for the electric fields has the form $\boldsymbol{D}_{\rm LSP}(\omega;\boldsymbol{r},\boldsymbol{r}')=\sum_n D_n(\omega)\boldsymbol{E}_n(\boldsymbol{r})\boldsymbol{E}_n(\boldsymbol{r}')$.

We now note that, in the quasistatic regime, the frequency and coordinate dependencies in the LSP Green's function can be separated out. Using the Gauss equation (3) in the integral form $\int dV\varepsilon'(\omega_n,\boldsymbol{r})\boldsymbol{E}_n^2(\boldsymbol{r})=0$, the volume integral in Eq. (6) can be presented as

$$\int dV\varepsilon(\omega,\boldsymbol{r})\boldsymbol{E}_n^2(\boldsymbol{r})=[\varepsilon(\omega)-\varepsilon'(\omega_n)]\int dV_{\rm m}\boldsymbol{E}_n^2(\boldsymbol{r}), \tag{7}$$

where integration in the right-hand side is carried over the *metal* volume $V_{\rm m}$, while the dielectric regions' contributions, characterized by constant permittivities, cancel each other out. The LSP Green's function takes the form

$$\boldsymbol{D}_{\rm LSP}(\omega;\boldsymbol{r},\boldsymbol{r}')=-\sum_n\frac{4\pi}{\int dV_{\rm m}\boldsymbol{E}_n^2}\frac{\boldsymbol{E}_n(\boldsymbol{r})\boldsymbol{E}_n(\boldsymbol{r}')}{\varepsilon(\omega)-\varepsilon'(\omega_n)}, \tag{8}$$

which represents the basis for our further analysis of the optical properties of metal nanostructures. Note that near the LSP pole the denominator of Eq. (8) can be expanded as $\varepsilon(\omega)-\varepsilon'(\omega_n)=[\partial\varepsilon'(\omega_n)/\partial\omega_n](\omega-\omega_n+i\gamma_n/2)$, where $\gamma_n=2\varepsilon''(\omega_n)/[\partial\varepsilon'(\omega_n)/\partial\omega_n]$ is the LSP decay rate [3], and we recover the Lorentzian approximation for the LSP Green's function [40–42].

III. LDOS, DOS, AND MODE VOLUME

Using representation (8) for the LSP Green's function, we can establish some general spectral properties of LSPs. In the following, we consider metal nanostructures of arbitrary shape in a dielectric medium with permittivity ε_d (we set $\varepsilon_d=1$ for now). We assume that ω lies in the plasmonics frequency domain, i.e., $|\varepsilon''(\omega)/\varepsilon'(\omega)|\ll 1$, and so the LSP quality factor $Q_n=\omega_n/\gamma_n=\omega_n[\partial\varepsilon'(\omega_n)/\partial\omega_n]/2\varepsilon''(\omega_n)$ is sufficiently large [3]. An important quantity that is critical in many applications is the local density of states (LDOS), which describes the number of LSP states in the unit volume and frequency interval:

$$\rho(\omega,\boldsymbol{r})=\frac{1}{2\pi^2\omega}{\rm Im\,Tr}\boldsymbol{D}_{\rm LSP}(\omega;\boldsymbol{r},\boldsymbol{r})=\sum_n\rho_n(\omega,\boldsymbol{r}). \tag{9}$$

Here, $\rho_n(\omega,\boldsymbol{r})$ is the LDOS for an individual LSP mode which, using the Green's function (8), takes the form

$$\rho_n(\omega,\boldsymbol{r})=\frac{2}{\pi\omega}\frac{\boldsymbol{E}_n^2(\boldsymbol{r})}{\int dV_{\rm m}\boldsymbol{E}_n^2}{\rm Im}\left[\frac{-1}{\varepsilon(\omega)-\varepsilon'(\omega_n)}\right]. \tag{10}$$

Integration of the LDOS over the volume yields the LSP density of states (DOS) $\rho_n(\omega)=\int dV\rho_n(\omega,\boldsymbol{r})$, describing the number of LSP states per unit frequency interval. To elucidate the distribution of LSP states in the system, let us compare the LSP DOS inside the metal, $\rho_n^{\rm m}(\omega)=\int dV_{\rm m}\rho_n(\omega,\boldsymbol{r})$, and in the surrounding dielectric medium, $\rho_n^{\rm d}(\omega)=\int dV_{\rm d}\rho_n(\omega,\boldsymbol{r})$. From Eq. (10), $\rho_n^{\rm m}(\omega)$ is readily obtained as

$$\rho_n^{\rm m}(\omega)=\frac{2}{\pi\omega}{\rm Im}\left[\frac{-1}{\varepsilon(\omega)-\varepsilon'(\omega_n)}\right]. \tag{11}$$

To evaluate $\rho_n^{\rm d}(\omega)$, we use the Gauss equation to present the integral over the dielectric region outside the metal as $\int dV_{\rm d}\boldsymbol{E}_n^2=-\varepsilon'(\omega_n)\int dV_{\rm m}\boldsymbol{E}_n^2$, yielding

$$\rho_n^{\rm d}(\omega)=\frac{2}{\pi\omega}{\rm Im}\left[\frac{\varepsilon'(\omega_n)}{\varepsilon(\omega)-\varepsilon'(\omega_n)}\right]. \tag{12}$$

Since for typical LSP frequencies $|\varepsilon'(\omega_n)|\gg 1$, we have $\rho_n^{\rm d}(\omega)=|\varepsilon'(\omega_n)|\rho_n^{\rm m}(\omega)\gg\rho_n^{\rm m}(\omega)$, implying that the LSP states are primarily distributed *outside* the metal. The full LSP DOS $\rho_n(\omega)=\rho_n^{\rm m}(\omega)+\rho_n^{\rm d}(\omega)$ has the form

$$\rho_n(\omega)=\frac{2}{\pi\omega}{\rm Im}\left[\frac{\varepsilon'(\omega_n)-1}{\varepsilon(\omega)-\varepsilon'(\omega_n)}\right], \tag{13}$$

which is valid for *any* nanostructure shape.

Let us now evaluate the number of LSP states per mode, $N_n=\int d\omega\rho_n(\omega)$. Performing the frequency integration in the Lorentzian approximation, we obtain

$$N_n=\frac{2|\varepsilon'(\omega_n)-1|}{\omega_n\partial\varepsilon'(\omega_n)/\partial\omega_n}. \tag{14}$$

For the Drude form of $\varepsilon(\omega)$, Eq. (14) yields $N_n\approx 1$, implying that the LSP states saturate the mode's oscillator strength. However, for the experimental dielectric function, N_n can be

substantially below its maximal value, which has implications for the optical spectra (see below).

Another important quantity that characterizes the field confinement is the LSP mode volume $\mathcal{V}_n$, which is related to the LDOS as $\mathcal{V}_n^{-1} = \rho_n(\boldsymbol{r}) = \int d\omega \rho_n(\omega, \boldsymbol{r})$, where $\rho_n(\boldsymbol{r})$ is the LSP spatial density [40,41]. Performing the frequency integration, we obtain

$$\frac{1}{\mathcal{V}_n} = \int d\omega \rho_n(\omega, \boldsymbol{r}) = \frac{2\boldsymbol{E}_n^2(\boldsymbol{r})}{[\omega_n \partial \varepsilon'(\omega_n)/\partial\omega_n] \int dV_{\rm m} \boldsymbol{E}_n^2}. \quad (15)$$

While the LSP mode volume is a *local* quantity that can be very small [i.e., the density $\rho_n(\boldsymbol{r})$ can be very large] at hot spots, its integral is bound as $\int dV/\mathcal{V}_n = N_n \leqslant 1$.

IV. OPTICAL POLARIZABILITY

Consider now a metal nanostructure in the incident EM field $\boldsymbol{E}_{\rm in} e^{-i\omega t}$ that is nearly uniform on the system scale. The system's induced dipole moment is obtained by volume integration of the electric polarization vector, $\boldsymbol{p}(\omega) = \chi(\omega) \int dV_{\rm m} \boldsymbol{E}(\omega, \boldsymbol{r})$, where $\boldsymbol{E}(\omega, \boldsymbol{r})$ is the local field inside the metal, given by

$$\boldsymbol{E}(\omega, \boldsymbol{r}) = \boldsymbol{E}_{\rm in} + \chi(\omega) \int dV'_{\rm m} \boldsymbol{D}_{\rm LSP}(\omega; \boldsymbol{r}, \boldsymbol{r}') \boldsymbol{E}_{\rm in}. \quad (16)$$

Using the LSP Green's function (8), we obtain

$$\boldsymbol{E}(\omega, \boldsymbol{r}) = \boldsymbol{E}_{\rm in} - \sum_n c_n \boldsymbol{E}_n(\boldsymbol{r}) \frac{\varepsilon(\omega) - 1}{\varepsilon(\omega) - \varepsilon'(\omega_n)}, \quad (17)$$

where the coefficient c_n is given by

$$c_n = \frac{\int dV_{\rm m} \boldsymbol{E}_n \cdot \boldsymbol{E}_{\rm in}}{\int dV_{\rm m} \boldsymbol{E}_n^2}. \quad (18)$$

Expanding the incident field $\boldsymbol{E}_{\rm in}$ in Eq. (17) over the LSP eigenmodes as $\boldsymbol{E}_{\rm in} = \sum_n c_n \boldsymbol{E}_n(\boldsymbol{r})$, we obtain the local field inside the metal as

$$\boldsymbol{E}(\omega, \boldsymbol{r}) = -\sum_n c_n \boldsymbol{E}_n(\boldsymbol{r}) \frac{\varepsilon'(\omega_n) - 1}{\varepsilon(\omega) - \varepsilon'(\omega_n)}. \quad (19)$$

Integrating Eq. (19) over the system volume, multiplying the result by $\chi(\omega) = [\varepsilon(\omega) - 1]/4\pi$, and using Eq. (18), we obtain the plasmonic system's induced dipole moment as $\boldsymbol{p}(\omega) = \sum_n \boldsymbol{\alpha}_n(\omega) \boldsymbol{E}_{\rm in}$, where

$$\boldsymbol{\alpha}_n = |\chi'(\omega_n)| \frac{\left(\int dV_{\rm m} \boldsymbol{E}_n\right)\left(\int dV_{\rm m} \boldsymbol{E}_n\right)}{\int dV_{\rm m} \boldsymbol{E}_n^2} \frac{\varepsilon(\omega) - 1}{\varepsilon(\omega) - \varepsilon'(\omega_n)} \quad (20)$$

is the LSP mode polarizability tensor [here, $\varepsilon'(\omega_n) - 1 = -4\pi|\chi'(\omega_n)|$]. We now introduce the LSP mode polarization unit vector as $\boldsymbol{e}_n = \int dV_{\rm m} \boldsymbol{E}_n / |\int dV_{\rm m} \boldsymbol{E}_n|$ and the *effective* system volume V_n as

$$V_n = V_{\rm m} |\chi'(\omega_n)| s_n, \quad s_n = \frac{\left(\int dV_{\rm m} \boldsymbol{E}_n\right)^2}{V_{\rm m} \int dV_{\rm m} \boldsymbol{E}_n^2}. \quad (21)$$

Then, using Eqs. (20) and (21), we obtain the polarizability tensor $\boldsymbol{\alpha}_n(\omega) = \alpha_n(\omega) \boldsymbol{e}_n \boldsymbol{e}_n$, where the scalar polarizability $\alpha_n(\omega)$ is given by Eq. (2).

The parameter s_n in the effective volume (21) depends on the system geometry and characterizes the strength of LSP coupling to the external EM field. Namely, it describes the relative variation of the LSP mode field inside the metal structure, while being independent of its overall amplitude. For the dipole LSP modes, which have no nodes inside the nanostructure, s_n is nearly independent of the metal volume. For nanoparticles of spherical or spheroidal shape, its exact value is $s_n = 1$ [39], while smaller values $s_n \lesssim 1$ are expected for other geometries. For higher-order LSP modes, whose electric fields oscillate inside the structure and, hence, have small overlap with the incident field, the parameter s_n is small.

The polarizability (2) is valid for small nanostructures characterized by weak LSP radiation damping as compared to the Ohmic losses in metal. For larger systems, to satisfy the optical theorem, the LSP radiation damping must be included by considering the system's interaction with the radiation field, which leads to the replacement $\alpha_n \to \alpha_n[1 - (2i\omega^3/3c^3)\alpha_n]^{-1}$, where c is the speed of light [43,44]. For such systems, after restoring the permittivity of surrounding medium ε_d, the scalar polarizability takes the form

$$\alpha_n(\omega) = V_n \frac{\varepsilon(\omega) - \varepsilon_d}{\varepsilon(\omega) - \varepsilon'(\omega_n) - \frac{2i}{3} k^3 V_n [\varepsilon(\omega) - \varepsilon_d]}, \quad (22)$$

where $k = \sqrt{\varepsilon_d}\omega/c$ is the light wave vector, while the system effective volume is now given by

$$V_n = V_{\rm m} |\varepsilon'(\omega_n)/\varepsilon_d - 1| s_n/4\pi. \quad (23)$$

The optical polarizability (22) is the central result of this Letter which permits accurate description of optical spectra for diverse plasmonic structures, including those of irregular shape, using, as input, only the basic system parameters and the LSP frequency. In terms of α_n, the extinction and scattering cross sections have the form [44]

$$\sigma_{\rm ext}(\omega) = \frac{4\pi\omega}{c} |\epsilon_n|^2 \alpha_n''(\omega), \; \sigma_{\rm sc}(\omega) = \frac{8\pi\omega^4}{3c^4} |\epsilon_n|^2 |\alpha_n(\omega)|^2, \quad (24)$$

where $\epsilon_n = \boldsymbol{e}_n \cdot \boldsymbol{E}_{\rm in}/|\boldsymbol{E}_{\rm in}|$ is the LSP polarization relative to the incident light.

Note that Eq. (22) reproduces the known analytical results for nanostructures of simple shapes. For a nanosphere of radius a, we have $s_n = 1$, $\varepsilon'(\omega_n) = -2$, and we recover Eq. (1) with the effective volume $V_n = a^3$, which is significantly smaller than the system volume. The polarizability (22) also matches the known result for spheroidal nanoparticles [39]. For metal structures with multiple LSP resonances, including porous structures [45], the polarizability tensor is $\boldsymbol{\alpha}(\omega) = \sum_n \alpha_n(\omega) \boldsymbol{e}_n \boldsymbol{e}_n$, where V_n can now be considered as fitting parameters.

Finally, the universal form (22) for the optical polarizability is valid for metal nanostructures embedded in dielectric medium. For more complex layered systems, including core-shell structures, the corresponding expressions for polarizability are more cumbersome and, importantly, no

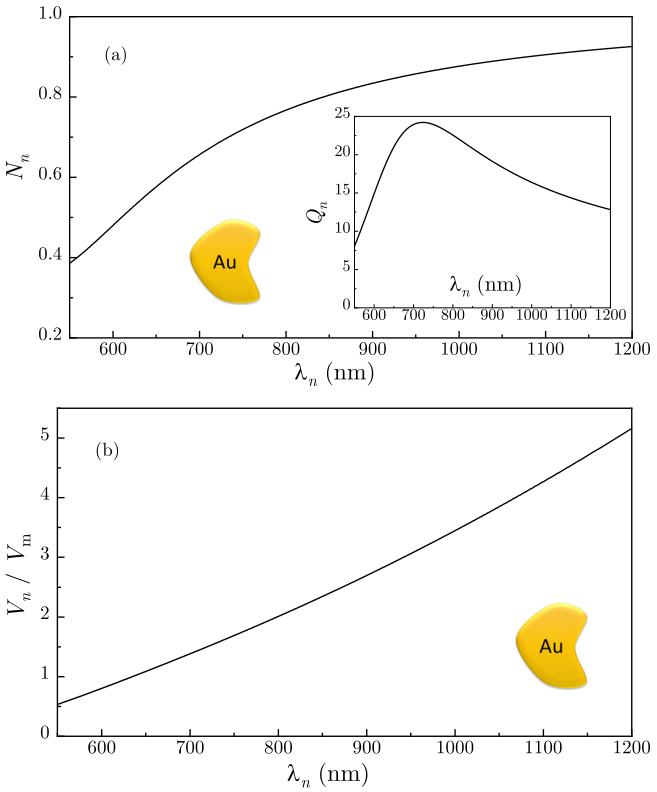

FIG. 1. (a) The number of LSP states for Au nanostructures is plotted against the LSP wavelength. Inset: The LSP quality factor wavelength dependence. (b) The normalized effective volume is plotted against the LSP wavelength.

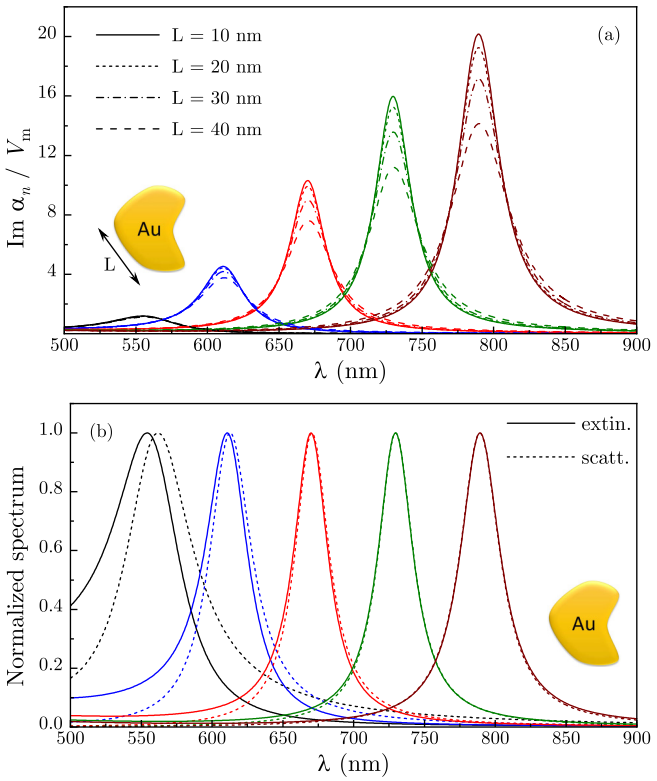

FIG. 2. (a) The imaginary part of polarizability for various Au structures is shown at different LSP wavelengths. (b) The normalized extinction and scattering spectra are shown for $L = 30$ nm structures.

longer universal, i.e., the lineshape of optical spectra now depends explicitly (not just via the LSP frequency) on the system geometry.

V. NUMERICAL RESULTS

Below we present the results of numerical calculations for small gold nanostructures to illustrate some general features of the LSP optical spectra that are common for any system geometry (we use the experimental gold dielectric function and set $s_n = 1$). In Fig. 1, we plot the number of LSP states per mode N_n and the effective volume V_n against the LSP wavelength λ_n in the interval from 550 to 1200 nm, i.e., for energies below the interband transitions onset in gold. With increasing λ_n, as the system enters the Drude regime, N_n increases, albeit slowly, towards its maximal value [see Fig. 1(a)]. However, for typical LSP wavelengths from 550 to 800 nm, N_n remains substantially below its maximal value, implying the important role of interband transitions even for energies well below the onset. Notably, N_n does *not* follow the LSP quality factor Q_n, shown in the inset, which peaks at $\lambda_n \approx 700$ nm due to the minimum of ε'' for gold at this wavelength. To elucidate the effect of system geometry, in Fig. 1(b), we plot the effective volume V_n normalized by the metal volume V_m in the same LSP wavelength interval. The normalized effective volume increases about *tenfold* from $\lambda_n = 550$ nm, roughly corresponding to the LSP wavelength in the gold nanosphere, to $\lambda_n = 1200$ nm, typical for LSPs in elongated particles with large aspect ratio. Since $V_n/V_m \approx |\chi'(\omega_n)|$, this implies that, for nanostructures of different shape but the *same* metal volume, both the lineshape and peak amplitude of the optical spectra are determined by the LSP resonance position.

In Fig. 2, we show the optical spectra of gold nanostructures in water ($\varepsilon_d = 1.77$) for different values of characteristic size L and, accordingly, of metal volume $V_m = L^3$, calculated using Eqs. (22)–(24) at the LSP wavelength values 550, 610, 670, 730, and 790 nm. The imaginary part of polarizability normalized by the metal volume increases sharply with the LSP wavelength [see Fig. 2(a)], consistent with the effective volume increase in Fig. 1(b). For larger structures, the LSP peak amplitudes of $\alpha_n''(\omega)/V_m$ drop due to the radiation damping. Although for full $\alpha_n''(\omega)$ such a decrease would be masked by larger V_m values, it is clear that, for the *same* metal volume, radiation damping is stronger for long-wavelength LSPs since it is determined by the effective volume V_n [see Eq. (22)].

In Fig. 2(b), we plot the extinction and scattering spectra, normalized by their respective maxima, for $L = 30$ nm gold nanostructures calculated for the same LSP wavelengths as in Fig. 2(a). For shorter wavelengths (<700 nm), the scattering spectra exhibit *apparent* redshift relative to the extinction spectra. Note that, for such system size, the extinction is dominated by the absorption, implying the prominent role of non-LSP excitations in this frequency region. This behavior is consistent with a relatively low fraction (about 50% at such wavelengths) of the LSP states per mode [see Fig. 1(a)]. In the Drude regime (larger LSP wavelengths), the difference

between the extinction and scattering spectra disappears as the LSP states saturate the oscillator strength.

In summary, we have developed an analytical model for optical polarization of plasmonic nanostructures of arbitrary shape whose characteristic size is below the diffraction limit. For such systems, the lineshape of optical spectra is determined by the metal dielectric function and LSP frequency while their amplitude depends on the system effective volume that increases with the LSP wavelength. We have also established some general spectral properties of the LSPs valid for any system geometry.

ACKNOWLEDGMENTS

This work was supported in part by NSF Grants No. DMR-2000170, No. DMR-1856515, and No. DMR-1826886.

[1] S. A. Maier and H. A. Atwater, J. Appl. Phys. **98**, 011101 (2005).
[2] E. Ozbay, Science **311**, 189 (2006).
[3] M. I. Stockman, in *Plasmonics: Theory and Applications*, edited by T. V. Shahbazyan and M. I. Stockman (Springer, New York, 2013).
[4] E. C. Le Ru and P. G. Etchegoin, *Principles of Surface-Enhanced Raman Spectroscopy* (Elsevier, Amsterdam, 2009).
[5] E. Dulkeith, A. C. Morteani, T. Niedereichholz, T. A. Klar, J. Feldmann, S. A. Levi, F. C. J. M. van Veggel, D. N. Reinhoudt, M. Moller, and D. I. Gittins, Phys. Rev. Lett. **89**, 203002 (2002).
[6] O. Kulakovich, N. Strekal, A. Yaroshevich, S. Maskevich, S. Gaponenko, I. Nabiev, U. Woggon, and M. Artemyev, Nano Lett. **2**, 1449 (2002).
[7] P. Anger, P. Bharadwaj, and L. Novotny, Phys. Rev. Lett. **96**, 113002 (2006).
[8] S. Kühn, U. Hakanson, L. Rogobete, and V. Sandoghdar, Phys. Rev. Lett. **97**, 017402 (2006).
[9] F. Tam, G. P. Goodrich, B. R. Johnson, and N. J. Halas, Nano Lett. **7**, 496 (2007).
[10] R. Bardhan, N. K. Grady, J. R. Cole, A. Joshi, and N. J. Halas, ACS Nano **3**, 744 (2009).
[11] T. Ming, L. Zhao, Z. Yang, H. Chen, L. Sun, J. Wang, and C. Yan, Nano Lett. **9**, 3896 (2009).
[12] V. N. Pustovit and T. V. Shahbazyan, Phys. Rev. Lett. **102**, 077401 (2009).
[13] J. Bellessa, C. Bonnand, J. C. Plenet, and J. Mugnier, Phys. Rev. Lett. **93**, 036404 (2004).
[14] Y. Sugawara, T. A. Kelf, J. J. Baumberg, M. E. Abdelsalam, and P. N. Bartlett, Phys. Rev. Lett. **97**, 266808 (2006).
[15] G. A. Wurtz, P. R. Evans, W. Hendren, R. Atkinson, W. Dickson, R. J. Pollard, A. V. Zayats, W. Harrison, and C. Bower, Nano Lett. **7**, 1297 (2007).
[16] N. T. Fofang, T.-H. Park, O. Neumann, N. A. Mirin, P. Nordlander, and N. J. Halas, Nano Lett. **8**, 3481 (2008).
[17] T. K. Hakala, J. J. Toppari, A. Kuzyk, M. Pettersson, H. Tikkanen, H. Kunttu, and P. Torma, Phys. Rev. Lett. **103**, 053602 (2009).
[18] A. Manjavacas, F. J. Garcia de Abajo, and P. Nordlander, Nano Lett. **11**, 2318 (2011).
[19] A. Salomon, R. J. Gordon, Y. Prior, T. Seideman, and M. Sukharev, Phys. Rev. Lett. **109**, 073002 (2012).
[20] A. Gonzalez-Tudela, P. A. Huidobro, L. Martin-Moreno, C. Tejedor, and F. J. Garcia-Vidal, Phys. Rev. Lett. **110**, 126801 (2013).
[21] T. Antosiewicz, S. P. Apell, and T. Shegai, ACS Photonics **1**, 454 (2014).
[22] A. De Luca, R. Dhama, A. R. Rashed, C. Coutant, S. Ravaine, P. Barois, M. Infusino, and G. Strangi, Appl. Phys. Lett. **104**, 103103 (2014).
[23] T. V. Shahbazyan, Nano Lett. **19**, 3273 (2019).
[24] D. J. Bergman and M. I. Stockman, Phys. Rev. Lett. **90**, 027402 (2003).
[25] M. I. Stockman, Nat. Photonics **2**, 327 (2008).
[26] M. A. Noginov, G. Zhu, A. M. Belgrave, R. Bakker, V. M. Shalaev, E. E. Narimanov, S. Stout, E. Herz, T. Suteewong, and U. Wiesner, Nature (London) **460**, 1110 (2009).
[27] T. V. Shahbazyan, ACS Photonics **4**, 1003 (2017).
[28] K. A. Willets and R. P. van Duyne, Annu. Rev. Phys. Chem. **58**, 267 (2007).
[29] A. B. Taylor and P. Zijlstra, ACS Sens. **2**, 1103 (2017).
[30] J. Zhou, A. I. Chizhik, S. Chu, and D. Jin, Nature (London) **579**, 41 (2020).
[31] S. Link, M. B. Mohamed, and M. A. El-Sayed, J. Phys. Chem. B **103**, 3073 (1999).
[32] K. L. Kelly, E. Coronado, L. L. Zhao, and G. C. Schatz, J. Phys. Chem. B **107**, 668 (2003).
[33] I. O. Sosa, C. Noguez, and R. G. Barrera, J. Phys. Chem. B **107**, 6269 (2003).
[34] P. K. Jain, K. S. Lee, I. H. El-Sayed, and M. A. El-Sayed, J. Phys. Chem. B **110**, 7238 (2006).
[35] C. Noguez, J. Phys. Chem. C **111**, 3806 (2007).
[36] R. Yu, L. M. Liz-Marzan, and F. J. Garcia de Abajo, Chem. Soc. Rev. **46**, 6710 (2017).
[37] J. Olson, S. Dominguez-Medina, A. Hoggard, L.-Y. Wang, W.-S. Chang, and S. Link, Chem. Soc. Rev. **44**, 40 (2015).
[38] R. Calvo, A. Thon, A. Saad, A. Salvador-Matar, M. Manso-Silvan, O. Ahumada, and V. Pini, Sci. Rep. **12**, 17231 (2022).
[39] See Supplemental Material at http://link.aps.org/supplemental/10.1103/PhysRevA.107.L061503 for the derivation of the LSP Green's function and of the polarizability of spheroidal nanoparticles.
[40] T. V. Shahbazyan, Phys. Rev. Lett. **117**, 207401 (2016).
[41] T. V. Shahbazyan, Phys. Rev. B **98**, 115401 (2018).
[42] T. V. Shahbazyan, Phys. Rev. B **103**, 045421 (2021).
[43] R. Carminati, J. J. Greffet, C. Henkel, and J. M. Vigoureux, Opt. Commun. **261**, 368 (2006).
[44] L. Novotny and B. Hecht, *Principles of Nano-Optics* (Cambridge University Press, New York, 2012).
[45] C. Vidal, D. Sivun, J. Ziegler, D. Wang, P. Schaaf, C. Hrelescu, and T. A. Klar, Nano Lett. **18**, 1269 (2018).